1   **Efficient surrogate modeling methods for large-scale Earth system models based on**

2   **machine learning techniques**

4   **Dan Lu[1,*], Daniel Ricciuto[2]**

7   [1]Computational Sciences and Engineering Division, Climate Change Science Institute, Oak

8   Ridge National Laboratory, Oak Ridge, TN, USA;

9   [2]Environmental Sciences Division, Climate Change Science Institute, Oak Ridge National

10   Laboratory, Oak Ridge, TN, USA;

13   * Corresponding Author: Dan Lu, lud1@ornl.gov

19   March 2019

20   For Publication in Geoscientific Model Development

Abstract

Improving predictive understanding of Earth system variability and change requires data-model integration. Efficient data-model integration for complex models requires surrogate modeling to reduce model evaluation time. However, building a surrogate of a large-scale Earth system model (ESM) with many output variables is computationally intensive because it involves a large number of expensive ESM simulations. In this effort, we propose an efficient surrogate method capable of using a few ESM runs to build an accurate and fast-to-evaluate surrogate system of model outputs over large spatial and temporal domains. We first use singular value decomposition to reduce the output dimensions, and then use Bayesian optimization techniques to generate an accurate neural network surrogate model based on limited ESM simulation samples. Our machine learning based surrogate methods can build and evaluate a large surrogate system of many variables quickly. Thus, whenever the quantities of interest change such as a different objective function, a new site, and a longer simulation time, we can simply extract the information of interest from the surrogate system without rebuilding new surrogates, which significantly saves computational efforts. We apply the proposed method to a regional ecosystem model to approximate the relationship between 8 model parameters and 42660 carbon flux outputs. Results indicate that using only 20 model simulations, we can build an accurate surrogate system of the 42660 variables, where the consistency between the surrogate prediction and actual model simulation is 0.93 and the mean squared error is 0.02. This highly-accurate and fast-to-evaluate surrogate system will greatly enhance the computational efficiency in data-model integration to improve predictions and advance our understanding of the Earth system.

1   Introduction

Improving predictive understanding of Earth system variability and change requires data-model integration. For example, Bilionis et al. (2015) improved Community Land Model (CLM) prediction of crop productivity after model calibration; Müller et al. (2015) improved the CLM prediction of methane emission after parameter optimization; and Fox et al. (2009) and Lu et al. (2017) improved the terrestrial ecosystem model predictive credibility of carbon fluxes after uncertainty quantification. However, data-model integration methods are usually computationally expensive involving a large ensemble of model simulations, which prohibits their application to complex Earth system models (ESMs) with lengthy simulation time. To reduce computational costs, surrogate modeling is widely used (Razavi et al., 2012; Gong et al, 2015; Ray et al., 2015; Huang et al., 2016, Lu et al., 2018; Ricciuto et al., 2018). The surrogate model, which is a set of mathematical functions, approximates the actual simulation model based on pairs of simulation model input-output samples, and then replaces the simulation model in the data-model integration. As the ESMs evaluation is expensive, it is desired to use a limited number of ESM simulation samples to build an accurate surrogate. As the surrogate model needs to be calculated many times in data-model integration, it is required to build a fast-to-evaluate surrogate. In this study, we use a very few simulation model runs to build an accurate and fast evaluated surrogate system of a large scale problem based on advanced machine learning methods.

In Earth system modeling, we usually need to build a surrogate system of many output variables over large spatial and temporal domains. ESMs tend to be simulated in a regional or global scale with many grid cells for several years, producing a large number of output variables. In addition, ESMs are used to solve versatile scientific problems, so the quantities of interest

66   (QoIs) often change. Moreover, the development of a surrogate requires expensive ESM runs,

67   and a large number of runs are often needed to capture the complex model input-output

68   relationship. Therefore, it is reasonable to build a surrogate system for all possible model outputs

69   to reduce the efforts of rerunning ESMs for a new surrogate development when the QoIs change.

70   In this way, whenever we simulate the outputs in a new site or for additional sites, at a different

71   time or for a longer period, we can simply extract the information of interest from the large

72   surrogate system without spending extra efforts in building new surrogates, which significantly

73   saves the computational costs.

74   Building and evaluating a surrogate system of a large number of model outputs can be very

75   computationally intensive for almost all the surrogate methods. Polynomials and artificial neural

76   networks are widely used for surrogate modeling (Razavi et al., 2012; Viana et al., 2014).

77   Polynomial methods, such as polynomial regression and radial basis functions, need to solve

78   polynomial coefficients in the surrogate construction and to calculate matrix multiplications in

79   the surrogate evaluation. Using a pth-order polynomial to approximate a model with d

80   parameters, $M = (p+d)!/(p!d!)$ coefficients need to be solved, i.e., the number of coefficients

81   increases factorially fast with the parameter size and polynomial order. When d=40, a second-

82   order polynomial involves 861 coefficients and a third-order polynomial involves 12341

83   coefficients. ESMs have many uncertain parameters and a high-order polynomial is usually

84   needed to approximate complex ESMs, which can easily lead to a prohibitive number of model

85   evaluations, up to $\sim 10^5$, necessary to compute the polynomial coefficients. To reduce the

86   computational costs, some regularization techniques such as Bayesian compressive sensing have

87   been used (Sargsyan et al., 2014; Ricciuto et al., 2018). These regularization techniques can use a

88   few samples to solve a large number of coefficients (i.e., an underdetermined system) by

89   iteratively minimizing the L1 norm of the coefficient vector. But they usually perform

90   minimization once for one model output, so for a large model outputs problem, significant

91   computing effort is required. To reduce the computing burden in building polynomial-based

92   surrogates, we need to reduce the output dimensions.

93   Reducing the model output dimensions also improves computational efficiency in the

94   evaluation of the polynomial-based surrogates. For example, evaluating the third-order

95   polynomial-based surrogate of the model with 40 parameters and 300,000 outputs at 1 parameter

96   sample, we need to calculate two matrix multiplications where matrix A has the size [1, M] and

97   B has the size [M, Nout] and M =12341 and Nout=300,000. The surrogate evaluation takes about

98   90 seconds and most time is spent on loading the huge matrix. When Nout reduces to 20, the

99   surrogate evaluation quickly reduces to less than a second. Note that an ESM can easily have

100   more than 40 parameters and more than 300,000 model outputs. Even using the most advanced

101   supercomputers with GPUs, the data storage and loading are still a bottleneck. Thus, reducing

102   model output dimensions is necessary for both fast building and evaluating polynomial-based

103   surrogates.

104   Neural network (NN) assisted surrogate modeling also suffers from high computational

105   costs when applied to a large-scale problem with many QoIs. To approximate a complex ESM

106   with many outputs, a complicated NN with many wide hidden layers is usually needed to capture

107   the complex relationship between the model inputs and outputs, because each spatial and

108   temporal output variable is driven by different meteorological forcing such as air temperature,

109   humidity, wind speed, precipitation, and radiation. The full connections between nodes in the

110   input layer and the first hidden layer, between nodes of the hidden layers, and between nodes in

111   the last hidden layer and a large number of nodes on the output layer, involve a great amount of

112   NN weights and biases that need to be solved. For the same example discussed above, to

113   approximate the model with 40 parameters and 300,000 model outputs, an NN with two hidden

114   layers and each layer having 100 nodes has over 30 million weights and biases. Calculation of

115   these weights and biases requires many samples to train the NN for a good fit. Each training

116   sample involves one model evaluation. However, ESM simulation is time consuming, which

117   usually takes several hours or days and can be up to months or even years. A limited sample size

118   is not enough to train a deep and wide NN for convergence and a simple NN trained by a small

119   sample size may not capture underlying Earth systems accurately. Thus, reducing model output

120   dimensions is needed to advance the NN-based surrogate modeling. A small output size reduces

121   the width of the output layer and also simplifies the relationship between the model inputs and

122   outputs, so that a simple NN architecture can be appropriate and a small sample size can be

123   sufficient to accurately train the simple NN. In addition, a simple NN can also be fast evaluated

124   with small weight matrix multiplications.

125   In this work, we propose to use singular value decomposition (SVD) to reduce model

126   output dimensions, so as to improve the computational efficiency in both building and evaluating

127   the surrogates. ESM outputs usually show periodic changes along time and strong correlations

128   between locations, which promises a fast decay of singular values. So, we can use a small

129   number of singular value coefficients to capture a great amount of output information, enabling a

130   significant output dimension reduction. We use the NN for surrogate modeling, because

131   compared to polynomial methods, NNs have shown less difficulty in fitting highly nonlinear and

132   discontinuous functions which are usually observed in ESMs response surfaces. For example,

133   carbon flux state variables, such as gross primary productivity (GPP), are strongly affected by

134   vegetation related parameters. When the parameter samples cause zero vegetation growth, GPP

135   has zero values. Whereas when the parameter samples cause high vegetation growth, GPP has

136   large positive values. This leads to a discontinuous GPP response surface jumping from zeros to

137   nonzeros.

138   NNs theoretically can fit any functions, but their practical performance strongly depends

139   on the NN's architectures and hyperparameters. NN has many hyperparameters such as the

140   number of layers, number of nodes in each layer, type of activation functions, and learning rate

141   of the stochastic gradient descent optimization. A slight change in the hyperparameter value can

142   result in dramatically different NN performance. Development of a high-performing NN is time-

143   intensive and usually requires trial-and-error tuning by machine learning experts. In this work,

144   we use Bayesian optimization techniques to optimize the NN architecture and hyperparameters

145   so as to produce an accurate NN model for the training data. Bayesian optimization searches the

146   hyperparameter space to iteratively minimize the validation errors of the NN by balancing

147   exploration and exploitation (Shahriari et al., 2016). Researches suggested that Bayesian

148   hyperparameter optimization of NNs is more efficient than manual, random, or grid search with

149   better overall performance on test data and less time required for optimization (Bergstra et al.,

150   2011; Snoek et al., 2012). Bayesian optimization involves a large ensemble of NN fittings and it

151   is a sequential model-based optimization, thus, fast training of the NN models is important. Our

152   proposed SVD method can simplify the NN architecture so as to advance the NN training and

153   improve the Bayesian optimization performance.

154   In this effort, we propose an SVD-enhanced, Bayesian-optimized, and NN-based surrogate

155   method and aim to build an accurate and fast-to-evaluate surrogate system of a large-scale model

156   using a few model runs, so as to improve computational efficiency in surrogate modeling and

157   thus advance the data-model integration. We apply the method to a simplified land model in the

158   Energy Exascale Earth System Model (sELM) to improve the model predictive capability of

159   carbon fluxes. We build a surrogate system of 42660 model output variables which are annual

160   GPPs at 1422 locations simulated for 30 years. The sELM is a regional-scale terrestrial

161   ecosystem model that simulates terrestrial water, energy, and biogeochemical processes in

162   terrestrial surfaces. Simulation of sELM is important for improving our understanding of

163   ecosystem responses to climate change. However, sELM requires lengthy times for hydrologic

164   and carbon cycle equilibration, and these high computational costs limit the affordable number of

165   simulations in data-model integration thus resulting in poor model performance. The proposed

166   machine learning assisted surrogate method makes the sophisticated data-model integration

167   computationally feasible and promises an improvement of the sELM predictions.

168   The major contributions of this work are (1) using SVD to reduce model output

169   dimensions so as to improve computational efficiency in both building and evaluating an

170   accurate surrogate of a large-scale ESM; (2) using Bayesian optimization techniques to fast

171   generate an accurate NN-based surrogate; and (3) applying the proposed method to build a large

172   surrogate system of a regional-scale ESM to advance data-model integration. To our knowledge,

173   the method of using SVD to enhance surrogate modeling is novel and we have not seen the

174   application of Bayesian optimization to improve NN-based surrogates in Earth system modeling.

175   The paper is organized as follows. In section 2, we first describe the sELM, the model

176   parameters and the QoIs we build surrogates for; following that, we introduce the SVD, NNs,

177   and Bayesian optimization methods. In section 3, we apply the methods to the sELM and analyze

178   the surrogate accuracy. In section 4, we discuss strategies to improve surrogate accuracy and

179   investigate our method's performance in the application of these strategies. In section 5, we end

180   this paper by drawing our conclusions.

2   Materials and Methods

2.1   Description of sELM and related parameters

We developed a simplified version of Energy Exascale Earth System (E3SM) land model (ELM), or sELM, to simulate carbon cycle processes relevant for Earth system models in a computationally efficient framework. This framework allows us to perform large regional ensembles that are computationally infeasible using offline land surface models such as ELM. sELM is a combination of model elements from the Data Assimilation Linked Ecosystem Carbon model (DALEC; Williams et al., 2005) and the Community Land Model version 4.5 (CLM4.5; Oleson et al., 2013). sELM consists of five process-based submodels that simulate carbon fluxes between five major carbon pools using 49 overall parameters. Based on previous sensitivity analysis using ELM (Ricciuto et al., 2018), this study considers the most sensitive eight parameters associated with four out of the five submodels. We summarize all five process-based submodels and their interactions below and in Figure 1.

sELM consists of five major submodels: photosynthesis, autotrophic respiration, allocation, deciduous phenology, and decomposition. Photosynthesis is driven by the aggregate canopy model (ACM) from the DALEC, which itself is calibrated against the soil-plant-atmosphere model (Williams et al., 2005). ACM predicts GPP as a function of carbon dioxide concentration, leaf area index, maximum and minimum daily temperature, and photosynthetically active radiation. Here the GPP predicted by ACM is modified by BTRAN, which reduces GPP when soil water is insufficient to support transpiration. Because sELM does not predict soil moisture, BTRAN is calculated in a full ELM simulation and is fed into sELM as an input. ACM shares one parameter, the leaf carbon to nitrogen ratio (*leaf C:N*), with the

203   autotrophic respiration model and employs an additional parameter, the specific leaf area at the

204   top of the canopy (*slatop*).

205   The remaining four submodules are based on ELM. The autotrophic respiration model

206   computes the growth and maintenance respiration components and is controlled by four

207   parameters, the *leaf C:N*, the fine root carbon to nitrogen ratio (*froot C:N*), the base rate of

208   maintenance respiration (*br_mr*), and temperature sensitivity for maintenance respiration

209   (*q10_mr*). The allocation model partitions carbon to several vegetation carbon pools following

210   those in ELM: leaves, fine roots, live stem, dead stem, live coarse roots and dead coarse roots. In

211   the allocation model, we only consider one parameter, the fine root to leaf allocation ratio

212   (*froot_leaf*). The deciduous phenology model is used to predict the timing of budbreak and

213   senescence. It considers two parameters, the critical day length to initiate autumn senescence

214   (*crit_dayl*) and the number of accumulated growing degree days needed to initiate spring leaf-out

215   (*crit_onset_gdd*). The last submodel is a decomposition model that simulates heterotrophic

216   respiration and the decomposition of litter into soil organic matter using the converging trophic

217   cascade framework as in the CLM4.5 (Oleson et al., 2013). Because this study focuses on plant

218   carbon uptake, no uncertain parameters are considered in the decomposition model. In sELM,

219   nutrient feedbacks are not represented explicitly, however a constant nitrogen limitation factor is

220   included to downregulate photosynthetic uptake.

221   The sELM can simulate several carbon state and flux variables as shown in Figure 1 with

222   green shapes. GPP, which represents the total plant carbon uptake, is considered in this study.

223   Here we use sELM to predict annual GPP in deciduous forest systems in the eastern region of the

224   United States for 30 years between 1981-2010. The carbon state variables are spun up to steady

225   state by cycling the GSWP3 input meteorology (Kim et al., 2017) from 1981-2010 for 5 cycles,

226   and the 6th cycle is used as the output for our surrogate modeling study. The region of interest

227   covers 1422 land grid cells (locations) as shown in Figure 2. Given 30 outputs at each location

228   (annual values over 30 years), a total of 42660 GPP variables are simulated. The model uses one

229   plant functional type and the phenological drivers such as air temperature, solar radiation, vapor

230   pressure deficit, and CO_2 concentration are used as boundary conditions. One regional sELM run

231   takes about 24 hours on a single processor, which although much faster than ELM is still

232   computationally too expensive to be directly used in model-data integration studies. To improve

233   the computational efficiency in generating the sELM simulation samples to develop the surrogate

234   model, we use high performance computing to perform an ensemble of 2000 sELM model

235   simulations in parallel. The 2000 parameter input samples are randomly drawn from the

236   parameter space defined in Figure 3. The numerical ranges of these parameters are designed to

237   reflect their average values and broad uncertainties associated with the temperate deciduous

238   forest plant functional type. The output samples are sELM simulated GPPs at the 1422 locations

239   for 30 years. In the surrogate modeling, part of the 2000 input-output samples are used for

240   developing the surrogate and part of them are used to evaluate the surrogate accuracy, as

241   discussed in section 3.

242   **2.2   Efficient surrogate modeling methods**

243   In this section, we introduce our SVD-enhanced, Bayesian-optimized, and NN-based

244   surrogate methods. We first describe the SVD for reducing data dimensionality, then introduce

245   the NN techniques for building a surrogate model, and last depict the Bayesian optimization

246   algorithm for producing a high-performing NN-based surrogate.

2.2.1   Singular value decomposition for data compression

247

248   We build a surrogate system of model outputs by fitting a data matrix whose columns are

249   output variables and rows are output samples. For a model with 100000 output variables, the

250   columns of this matrix span a 100000-dimensional space. Encoding this matrix on a computer

251   takes quite a lot of memory and evaluating this matrix takes a large number of calculations. We

252   are interested in approximating this matrix with some low-rank matrix but remaining its most

253   information, so as to reduce data transfer and accelerate matrix calculation.

254   Singular value decomposition (SVD) decomposes a matrix $\mathbf{A}$ with size $m \times n$ into three

255   other matrices, $\mathbf{A} = \mathbf{U}\mathbf{S}\mathbf{V}^T$, where $\mathbf{U}$ is an $m \times m$ orthogonal matrix, $\mathbf{V}$ is an $n \times n$ orthogonal

256   matrix, and $\mathbf{S}$ is an $m \times n$ diagonal matrix saving singular values in descending order on the

257   diagonal. Truncated SVD keeps the K largest singular values and corresponding K column

258   vectors of $\mathbf{U}$ and K row vectors of $\mathbf{V}^T$ to form $\widetilde{\mathbf{A}} = \mathbf{U}_K \mathbf{S}_K \mathbf{V}_K^T$. The K-rank matrix $\widetilde{\mathbf{A}}$ has proven to

259   be the best approximation of $\mathbf{A}$ in minimizing the Frobenius norm of the difference between $\mathbf{A}$

260   and $\widetilde{\mathbf{A}}$ under the constraint of rank($\widetilde{\mathbf{A}}$) = K. In addition, the total of the first K singular values

261   divided by the sum of all the singular values is the percentage of information that those singular

262   values contain (i.e., the percentage of the total variance explained by those singular values). For

263   example, if we want to keep 90% of the data information, we just need to compute sums of K

264   largest singular values until we reach 90% of the sum and discard the rest. By dropping all but a

265   few singular values and then recomputing the approximated matrix, the SVD technique

266   compresses the data information and reduces data dimensions. When the matrix $\mathbf{A}$ shows strong

267   correlations between columns (variables), a low-rank matrix $\widetilde{\mathbf{A}}$ can make a very accurate

268   approximation of $\mathbf{A}$.

269   In this study, we use SVD to reduce training data dimensions. The training data matrix $\mathbf{A}$

270    $[m, n]$ for surrogate construction contains model output samples information. n columns are

271   output variables (e.g., the 42660 temporal and spatial GPPs in this work) and m rows are the

272   samples of these variables (e.g., the sELM simulation results of the 42660 GPPs for the m

273   parameter samples), and usually $n \gg m$ for expensive ESMs with many outputs. In

274   implementation, we first perform truncated SVD to get low-rank matrices $\mathbf{U}_K[m, K]$, $\mathbf{S}_K[K, K]$,

275   and $\mathbf{V}_K^T[K, n]$ with $K \ll n$, we then use the low-dimensional dataset $(\mathbf{V}_K^T \mathbf{A}^T)^T$ with reduced size m

276    $\times K$ as training data to build the surrogate model of the K largest singular value coefficients.

277   Next, we evaluate the surrogate model at q new data points to get results $\mathbf{Y}_{\text{new}}$ with size $q \times K$.

278   Lastly, we transform the predicted values back to its original size $q \times n$ through $\mathbf{Y}_{\text{new}} \mathbf{V}_K^T$ to obtain

279   the surrogate approximation of the n variables at the q new data points.

280   **2.2.2   Neural networks for surrogate modeling**

281   Artificial neural networks (NNs) consist of fully connected hierarchical layers with nodes

282   which can be flexibly used for function approximation (Yegnanarayana, 2009). The first layer is

283   the input layer and each node in the input layer represents one model input variable. The last

284   layer is the output layer and each node in the output layer represents one model output variable.

285   The layers between input and output layers are hidden layers which are used to approximate the

286   relationship between model inputs and outputs. When the relationship is complex, a complicated

287   NN with many wide hidden layers is usually needed. The input layer first assigns model

288   parameter values to its nodes. Then each node in the first hidden layer takes multiple weighted

289   inputs, applies the activation function to the summation of these inputs, and calculates the node's

290   value. Next, the second hidden layer takes the values on the first hidden layer nodes as inputs

291   and calculates its nodes' values in the same way. This process moves forward till we get values

292   of all nodes in the output layer, i.e., obtaining NN predictions for the given model parameter

293   input values. The nodes in each layer are fully connected to all the nodes in its previous and

294   subsequent layers. Each of these connections has an associated weight and bias. A complicated

295   NN results in a large number of weights. By tuning these weights and biases based on some

296   training data, we improve the NN approximation of the underlying simulation model.

297   NN uses stochastic gradient descent (SGD) method to optimize its weights and biases

298   (Bottou, 2012). SGD optimizes variables by minimizing some loss function based on the

299   function's gradients to these variables. The loss function is usually defined as the mean squared

300   error (MSE) between the NN predictions and model simulations for the same set of model

301   parameter samples in the training data. SGD iteratively updates the optimized variables at the

302   end of each training epoch. In the process, the learning rate, which specifies how aggressively

303   the optimization algorithm jumps between iterations, greatly affects the algorithm's performance

304   and has to be tuned. A small learning rate will take a long time to reach the optimum causing a

305   slow convergence, whereas a big learning rate will bounce around the optimum causing unstable

306   results and a difficult convergence. Using SGD to optimize a complex NN with many weights

307   requires a great amount of computational efforts and has difficulty in convergence. First, many

308   training data are required to tune a large number of weights. Small training data can easily cause

309   over-fitting, i.e., the NN "perfectly" fits the training data but performs badly on new data, thus

310   deteriorating the NN prediction accuracy. In addition, a large number of weights involve massive

311   matrix calculations in evaluating the loss function, slowing down the training process.

312   Furthermore, a complicated NN has difficulty in convergence and can easily get stuck in local

313   minima. In this work, we use SVD to reduce the model output dimensions, so as to decrease the

314   number of nodes in the output layer and simplify the NN architecture, thus reducing the size of

315   the weights and enabling a reasonable NN training from small training data, and ultimately

316   improving the computational efficiency.

2.2.3   Bayesian algorithms for NN hyperparameter optimization

318   NN involves a lot of hyperparameters that dramatically affect its performance such as the

319   number of layers, the number of nodes in each layer, and the learning rate of the SGD algorithm.

320   Hyperparameter optimization is needed to produce a high-performing NN. This requires

321   optimizing an objective function $f(x)$ over a tree-structured configuration spaces $x \in X$, where

322   some leaf variables (e.g., the number of nodes in the third hidden layer of an NN) are only well

323   defined when branch variables (e.g., a discrete choice of how many layers to use) take particular

324   values. In addition, the optimization not only optimizes discrete and continuous variables, but

325   also simultaneously choose which variables to optimize. When the NN is used for surrogate

326   modeling, the objective function is the NN accuracy of predicting some validation data. In this

327   case, the $f(x)$ does not have a simple closed form but can be evaluated at any arbitrary query

328   point x in the configuration space. For such optimization problem, a sequential search method is

329   needed, besides some inefficient grid search and random search approaches (Bergstra and

330   Bengio, 2012). The sequential search method starts with some random points in the search space,

331   and then iteratively evaluates new points based on NN predictions on previously evaluated

332   points. After N evaluations, we choose the optimal combination of the hyperparameters resulting

333   in the highest NN prediction accuracy. Among the sequential search algorithms, Bayesian

334   optimization is able to take advantage of full information provided by the history of the

335   optimization to improve the search efficiency.

336   Bayesian optimization first prescribes a prior belief over the possible objective functions

337   and then sequentially updates this prior distribution to posterior distributions as points are

338   evaluated via Bayesian posterior updating. The prior and posterior distributions are the

339   probabilistic model that approximates the unknown objective function we are optimizing. With

340   this probabilistic model, we can sequentially induce acquisition function that leverages the

341   uncertainty in the posterior to guide exploration of new data points for updating the model. The

342   acquisition function evaluates the utility of candidate points for the next evaluation of $f(x)$,

343   therefore the next iteration point x_{n+1} is selected by maximizing the acquisition function. As

344   more data information is incorporated to exploit the objective function, we get closer to find the

345   best estimate of the optimizer.

346   Dependent on the choice of the probabilistic model, we have different Bayesian

347   optimization algorithms (Shahriari et al., 2016). The Gaussian process approach, using the

348   Gaussian process as probabilistic model and expected improvement as acquisition function, has

349   been widely used for parameter optimization (Bardenet and Kegl, 2010; Rasmussen and

350   Williams, 2006; Niranjan et al., 2010). However, this approach has a few disadvantages when

351   applying to optimize NN hyperparameters. First, it does not work well for categorical variables

352   such as the type of activation functions in NN. Secondly, it selects new set of parameter points

353   based on the best evaluation data. However, NN usually involves randomization during the

354   training process. So, running NN with the same parameter values can lead to different

355   performance which suggests that our best point can be just lucky output for the specific setting of

356   randomness. Thirdly, Gaussian process itself involves several hyperparameters such as the kernel

357   of the covariance function; a good choice of these hyperparameters can significantly affect the

358   optimization but the selection of them is difficult. Lastly, the calculation of Gaussian process is

359   rather slow, especially for a large number of parameters search (Snoek et al., 2012).

360   In this work, we use tree-structured Parzen estimator (TPE) for NN hyperparameter

361   optimization (Bergstra, et al., 2013). TPE first performs a few iterations of random search, and

362   then it divides collected parameter points into two groups. The first group contains points that

363   give best scores after evaluation, which can be the top 10-25% of all the points, and the second

364   group has all other points. Next, TPE finds a set of parameters that more likely to be in the first

365   group and less likely to be in the second group through the following steps: (1) estimate

366   likelihood probability for each of the two groups based on Parzen-window density estimators

367   (Archambeau et al., 2006); (2) sample a bunch of candidate points using the likelihood

368   probability from the first group; and (3) select the point having the largest probability ratio of

369   being in the first group to the second group as the next iteration point. Lastly, we continue the

370   searching till we hit the maximum evaluation and choose the optimal parameter combination that

371   gives the best NN accuracy on the validation data.

372   The TPE algorithm exhibits significant improvement over the classic hyperparameter

373   optimization methods. TPE works well for all types of NN hyperparameter variables; it considers

374   a set of top parameters to avoid the influence from NN randomization; its implementation is

375   straightforward and has no associated hyperparameters for specification; and the calculation of

376   TPE is computationally fast (Bergstra et al., 2011).

377   **3   Results**

378   In this section, we present the results of building the surrogate system of 42660 GPP

379   variables of sELM. First, we demonstrate that our method using SVD can efficiently build and

380   evaluate a large surrogate system by comparing the results with and without application of SVD.

381   We then investigate the influence of NN's architecture on surrogate performance and show that

382 our method using hyperparameter optimization can fast generate an accurate NN. Last, we

383 evaluate surrogate accuracy on the large-scale spatial and temporal GPPs.

384   We consider three sets of data, the training data for fitting the NN, the validation data to

385 detect overfitting in the NN training and to select the best-performing NN in the hyperparameter

386 optimization, and the test data to evaluate the NN prediction accuracy. Each data set contains

387 pairs of parameter and GPP samples. The parameter samples are randomly drawn from the

388 parameter space defined in Figure 3. To assess the effectiveness of our proposed surrogate

389 method for a small data set, we consider only 20 training data (Figure 3). The validation data is

390 chosen as 0.3 fractions of the training data. The NN model will not train on the validation data

391 but evaluate the loss function on them at the end of each epoch. In each epoch, the training data

392 is shuffled, and the validation data are always selected from the last 0.3 fraction. Precisely, we

393 only use 14 samples to tune NN weights. Attribute to shuffling, these 14 samples can be a

394 different subset from the 20 training data in each epoch, thus we sufficiently explore the limited

395 20 data information for building the surrogates. We use 1000 test data (Figure 3) to evaluate the

396 NN prediction accuracy, which makes a reasonable assessment of our proposed method within

397 an affordable computational cost. Note that the 1000 test data are not needed for building the

398 surrogates but used to demonstrate the effectiveness and efficiency of our method. When using

399 our method to build the surrogates of the 42660 GPPs, only 20 sELM model simulations are

400 used.

401   We define the loss function as the mean squared error (MSE) between the NN predictions

402 and the sELM simulations based on the parameter samples for training. We use Adam algorithm

403 (Kingma and Ba, 2015) for stochastic optimization of NN and run it for 800 epochs to minimize

404 the loss function and update NN weights. Adam has been shown a superior stochastic

405   optimization algorithm in training NN (Basu et al., 2018). There is no right answer for the

406   optimal number of epochs. A small number of epochs could result in underfitting and a large

407   number of epochs may lead to overfitting. Here we consider a large number of epochs and in the

408   meantime use early stopping to avoid overfitting. During the training, when there is no

409   improvement of loss functions for the validation data in 100 epochs, we stop the training and

410   choose the weights at the epoch resulting in the smallest loss function of the validation data as

411   the optimal weights and the associated NN as the best trained NN under the given setting.

412   We then use the trained NN to predict the 1000 test data and compare the predictions with

413   the corresponding sELM simulation results to evaluate the NN accuracy. We define two metrics

414   for evaluation, the MSE and the coefficient of determination. The MSE computes the expected

415   value of the squared prediction errors; the small the MSE value is, the better the prediction. The

416   coefficient of determination, also called R^2 score, measures how well the unobserved data are

417   likely to be predicted by the NN model. Denote $\hat{y}_i$ as the NN prediction of the *ith* sample and y_i

418   as the corresponding sELM simulation, the R^2 score estimated over N_s samples is defined as

419    $R^2 = 1 - \frac{\sum_{i=1}^{N_s}(y_i - \hat{y}_i)^2}{\sum_{i=1}^{N_s}(y_i - \bar{y}_i)^2}$, where $\bar{y} = \frac{1}{N_s}\sum_{i=1}^{N_s} y_i$. Best possible value of R^2 score is 1.0, indicating

420   that the NN can perfectly predict the test data. R^2 score can be negative indicating the model is

421   arbitrarily poor. A constant model gets a R^2 score of 0.0. Compared to MSE, the R^2 score

422   considers the variability of the data which provides a more reasonable measure.

423   **3.1   SVD reduces data dimensionality and improves surrogate efficiency**

424   We consider two scenarios when building the surrogate system of the 42660 GPP outputs;

425   Case I: building the surrogates of reduced data after SVD, and Case II: building the surrogates of

426   all GPPs directly. In Case I, we first apply SVD to reduce the training data dimensionality, then

427   build surrogates of the singular value coefficients, and last transfer the surrogate system back to

428   the original QoIs (i.e., the 42660 GPP variables).

429   The goal of this study is to develop a surrogate method that builds an accurate surrogate

430   system with small training data, so as to reduce the computational costs in simulating the

431   expensive ESMs. To demonstrate the effectiveness and efficiency of our method, we compare

432   the surrogate performance of the two cases in predicting the 1000 test data from two aspects: (1)

433   for the same number of training data, the predictive accuracy of the two surrogates, and (2) the

434   number of training data used to achieve the similar predictive accuracy.

435   Figure 4 shows the singular value decay of decomposition of the training data matrix

436   having 20 samples and 42660 GPP variables. The figure indicates that the singular values decay

437   very fast. The first 2 singular values drop about 1 magnitude, and the first 5 singular values can

438   capture 97% information of the training data matrix. To choose a suitable number of singular

439   value coefficients (Nsvd) to compress the training data and build a surrogate for, we consider a

440   series of Nsvds, where Nsvd=1, 5, 10, 15, and 20, and investigate their impact on NN

441   performance. To make a fair comparison, the same NN architectures are used for all Nsvd cases.

442   We consider a simple NN with 2 hidden layers and each hidden layer has 10 nodes. Figure 5

443   shows the prediction performance of the NNs based on the 20 training data. The figure indicates

444   that with considering only 1 singular value coefficient, the averaged MSE of the predictions is

445   about 0.053, and the NN model can fit the sELM simulation data well with the R^2 score of 0.83.

446   When 5 singular value coefficients are considered, the NN prediction accuracy improves with the

447   MSE of 0.02 and the R^2 score of 0.93. After Nsvd=5, the MSE and R^2 score have minor changes,

448   suggesting that for the limited 20 training data, Nsvd=5 is a good choice to compress the GPPs

449   and build a surrogate for. At this time, the surrogate error becomes dominant compared to the

450   SVD approximation error and including more than 5 singular value coefficients would barely

451   improve the NN prediction unless more training data are included to reduce the surrogate error.

452   In the following, we consider Nsvd=5 in Case I and compare its surrogate prediction

453   performance with Case II which builds surrogates for all GPPs directly.

454   In Case I, our method is able to use 20 training data to build a highly accurate surrogate of

455   42660 GPP variables with a small MSE of 0.02 and a high R^2 score of 0.93. The detailed NN

456   performance is explained in Figure 6(a) where the training and validation loss decays in building

457   the surrogates of the 5 singular value coefficients are plotted. The figure indicates that the loss

458   functions of the two data sets have similar decay, decreasing dramatically at the first 10 epochs

459   and then slowly decreasing to the end of training. The closely overlapped two lines in Figure 6(a)

460   suggest that the trained NN captures the relationship between sELM inputs and outputs pretty

461   well and can give reasonable predictions of GPPs for a given parameter sample.

462   To make a fair comparison, we use the same NN architecture in Case II as in Case I except

463   that the output layer of NN in Case II has all the 42660 GPPs and the output layer in Case I has

464   only 5 singular value coefficients. Figure 6(b) indicates that the simple NN with 20 hidden nodes

465   is not sophisticated enough to capture the complex relationship between the 8 inputs and 42660

466   outputs. As we can see in Figure 6(b), both training and validation losses are relatively high

467   suggesting an underfitting. The validation loss is always larger than the training loss suggesting

468   that the fitted NN does not generalize well and may result in poor performance in predicting new

469   data. Figure 7 shows R^2 scores of Case II in predicting the 1000 test data. The figure indicates

470   that the simple NN trained by 20 data in Case II has a very poor prediction accuracy with the R^2

471   score of only 0.05, close to a constant model's performance with a zero R^2 score. However, with

472   the same NN trained by the same 20 data, our SVD-based surrogate method can achieve a high

473   prediction accuracy with the R^2 score of 0.93. This demonstrates our method's capability in using

474   a few training samples to build an accurate surrogate model, greatly reducing the computational

475   costs in generating the expensive model simulation data.

476   On the other hand, the poor performance in Case II suggests that a wider and deeper NN is

477   needed when we consider the large outputs directly. We thus increase the nodes of each hidden

478   layer to 100 and use this complex NN with total 200 hidden nodes to approximate the

479   relationship of the 8 inputs and 42660 outputs in Case II. This complex NN blows up its

480   parameters (including weights and biases) to 4.3 million from 255 in Case I. To fit this wide NN

481   and calibrate its large parameters, 20 training data are way too small to get a reasonable fit. No

482   matter how we adjust the NN hyperparameters, we cannot get a stable solution in training. We

483   then increase the training data to 50, Figure 6(c) shows that the increased data greatly decrease

484   the training and validation losses and the validation loss is slightly higher than the training loss,

485   implying a good fit. Figure 7 indicates that the complex NN with 200 hidden nodes trained by 50

486   data in Case II significantly improves the prediction accuracy with the R^2 score of 0.73.

487   However, Case II's predictive performance is still worse than Case I which has the R^2 score of

488   0.93. We keep increasing the training data (Ntrain) to 100 and 200 in Case II. Figure 6(d) and (e)

489   indicate that the increase of training data brings the validation loss closer and closer to the

490   training loss making the fitted NN represent the underlying sELM better and better. Figure 7

491   shows that the nicely fitted NNs trained by large Ntrains lead to a high prediction accuracy. With

492   Ntrain=100, the R^2 score is about 0.89, and with Ntrain=200, the R^2 score is up to 0.95.

493   However, compared to Case I using 20 training data to get predictive R^2 score of 0.93, Case II

494   uses near 200 data to get the similar accuracy, increasing 10-fold computational costs. Note that,

495   each training data involves one sELM simulation and one regional sELM run takes about 24

496 hours on one processor. Thus, our SVD-based surrogate method greatly improves computational

497 efficiency in the accurate surrogate modeling.

498   Our method, in the means of simplifying NN architecture through data compression, not

499 only reduces the training data but also decreases the training time. Using 20 data to train a simple

500 NN with 255 parameters, our method takes about 4 seconds. In comparison, the traditional

501 surrogate method without data compression spends a great effort in training the complex NN

502 with 4.3 million parameters. As shown in Figure 7, Case II takes 270 seconds to fit the NN based

503 on 50 training data and 967 seconds for the 200 training data, showing a linear increase in

504 computing time. The long training time leads to high computational costs in NN hyperparameter

505 optimization where massive NN training are involved in searching the wide hyperparameter

506 space for a high-performing NN model, as discussed in the following section 3.2.

507 **3.2   NN's hyperparameter optimization improves surrogate accuracy**

508   NN has a large number of hyperparameters. Here we adjust 5 hyperparameters and use

509 Case I to investigate their influence on surrogate prediction accuracy. The 5 hyperparameters are,

510 the number of hidden layers (L) where we consider the most 3 hidden layers, the number of

511 nodes in hidden layer 1 (N1), in hidden layer 2 (N2), and in hidden layer 3 (N3), and the learning

512 rate (lr) of Adam optimization algorithm. We consider the following choices: L={2, 3}, N1={10,

513 20, 40, 60, 80, 100}, N2={10, 20, 40, 60, 80, 100}, N3={0, 10, 20, 40, 60, 80, 100}, and

514 lr=U[0.001, 0.1]. The first four hyperparameters are discrete variables and the last one, lr, is a

515 continuous variable with uniform distribution. The choice of L determines the selection of N3

516 showing a tree-like structure. We use tree-structured Parzen estimator (TPE) to search the 5

517 hyperparameter space and find a set of values that gives the best-performing NN. We fix the

518   activation function as ReLU (Agarap, 2018) which has been widely used and shown to produce

519   good NN predictions.

520   We use TPE to evaluate 100 sets of hyperparameters and the one giving the best validation

521   score, i.e., the smallest MSE on validation data, is chosen as the optimal hyperparameters.

522   Results indicate that the combination of N1=10, N2=10, N3=0, and lr=0.08 gives the best

523   validation score. To investigate the impact of hyperparameters on NN prediction accuracy, we

524   show the 100 sets of hyperparameters and their resulting R^2 scores in predicting the 1000 test

525   data in Figure 8. The figure indicates that different hyperparameter values result in dramatically

526   different NN performance. The prediction R^2 scores range from 0.66 to 0.93 where 32

527   hyperparameter sets have the R^2 scores over 0.90. The selected optimal NN producing the

528   smallest MSE on the validation data also gives the best prediction performance on the test data

529   with the R^2 score of 0.93. It is desired that the best NN model chosen by validation data gives the

530   best predictions, however, in practice it is not always the case, especially when the prediction

531   data deviates a lot from the validation data. Extrapolation is always a difficulty in surrogate

532   modeling and several researches are going on to improve the extrapolation accuracy (Gal, 2014).

533   Although NNs perform significantly different with different combination of

534   hyperparameters, the TPE algorithm can efficiently find the high-performing NNs based on

535   previous samples information. As shown in Figure 8, good-performing NNs prefer simple

536   architectures with 2 hidden layers, e.g., most blue lines have N3 of 0. After TPE finds a good

537   architecture of N1=10 and N2=10, it samples around this architecture in the hyperparameter

538   space to fine tune the learning rate till finds the most suitable lr of 0.08. This work considers 5

539   hyperparameters with limited choices, increasing the dimensions and possible choices of the

540   hyperparameters would make the search more thorough and could produce a better-performing

541 NN. Our surrogate method with SVD can accelerate the optimization process by reducing the

542 NN training time.

3.3 Evaluation of surrogate accuracy on large-scale spatial and temporal data

544 We, using only 20 expensive sELM runs, fast build an accurate surrogate system of 42660

545 GPPs at 1422 locations for 30 years. Therefore, for a data-model integration problem with the

546 QoIs within the spatial and temporal ranges, we can directly extract the information of interest

547 from the surrogate system to advance the analysis. The best-performing NN generated from our

548 method gives an overall accurate prediction of the 42660 GPPs with averaged MSE of 0.02 and

549 R^2 scores of 0.93. When using the subset of the surrogate system for data-model integration

550 studies, it is desired to analyze the surrogate accuracy at individual locations for specific times.

551 Figure 9 shows averaged R^2 scores over 30 years at 1422 locations. The figure indicates

552 that the surrogate accuracy is not uniformly good for all the locations. We observe that most

553 locations have R^2 scores above 0.9 with the best R^2 score of 0.96, and about 100 locations have

554 R^2 scores below 0.90 with the smallest R^2 score of 0.79. We highlight the locations having zero

555 GPP simulations in blue circles and find that these locations generally have poor predictions with

556 low R^2 scores. Connecting to Figure 2 where we label the locations in column-wise from south to

557 north and from west to east, we identify that those locations with zero GPPs are mostly located in

558 the north where the temperature is relatively low and annual GPPs tend to be zero for parameter

559 samples.

560 We pick 3 locations to closely evaluate the surrogate accuracy (Figure 9). Location 1046

561 has the best prediction with the highest R^2 score, location 1345 has the worst prediction

562 accuracy, and location 428 performs best among the locations with zero GPP simulations. Figure

563 10 shows annual GPP simulations based on sELM and NN-based surrogate in evaluating the

564   1000 test data for 30 years at the 3 locations. It can be seen that NN has difficulty in fitting zero

565   GPP data. At location 1046 where the annual GPPs are relatively high with positive values, NN

566   produces a great fit with a high R^2 score of 0.96 and a small MSE of 0.013. Location 1046

567   (Figure 2) is close to the lake where the variance in atmospheric drivers (e.g., temperature) is

568   moderated. This reduced variance leads to a smooth response surface of GPP for which NN can

569   easily build an accurate surrogate. In contrast, location 1345 has a large number of simulated

570   GPPs less than 1.0 including many zero GPPs. NN shows difficulty in predicting these small

571   GPPs resulting in a relatively poor performance with the R^2 score of 0.79. Location 1345 is

572   sitting in the north and has the lowest mean annual temperature, so the most parameter samples

573   cause low vegetation growth and small GPP values. Moreover, location 1345 is far away from

574   the lakes and has a large variation in atmospheric drivers. Since this location has a climate that is

575   at the extreme end of the range for deciduous forests, the model response is expected and

576   reasonable. However, this leads to a strong nonlinear response surface that casts difficulty in

577   surrogate modeling. In comparison, although location 428 is located in the north with some small

578   GPPs including zero values, it is also close to the lake which has a small variance in the

579   atmospheric drivers. Thus, the NN prediction performance in location 428 is not bad with the R^2

580   score of 0.91.

581   Figure 11 plots the averaged R^2 scores over all locations for 30 years. The R^2 scores have

582   small fluctuations between 0.93 and 0.94, displaying a uniformly good fit among the simulated

583   years. So, when using the surrogate model at any specific year for a data-model analysis, we

584   should be able to obtain a good approximation. In this study, we are considering annual GPPs.

585   Although the variation of atmospheric drivers between years has an impact on surrogate

586   accuracy, its influence is less strong compared to monthly GPPs, so a uniformly good fit among

587   years is expected.

588   Building a surrogate of the discontinuous response surface, e.g., vegetation turns from

589   alive to dead representing as the GPP jumps from nonzero to zero, is a difficulty for almost all

590   the state-of-the-art surrogate methods. Researches showed that, NNs, attribute to the layered

591   architecture and the nonlinear activation function, can show better performance compared to

592   other surrogate approaches (Luo and Lu, 2014; Razavi et al., 2012). To improve the surrogate

593   accuracy for strong nonlinear and discontinuous problems, one strategy is using physics-

594   informed domain decomposition methods to build surrogate models separately in different

595   response surface regimes. This strategy requires the surrogate methods strongly connecting to the

596   simulation model, and the methods are generally problem-specific requiring experts' interaction.

597   Another strategy is increasing the training data to explore complex problems. This strategy

598   requires an increase in computational costs for extra expensive model simulations. In the

599   following section 4, we investigate these two strategies and discuss their influence on surrogate

600   accuracy.

601   **4   Discussion**

602   ESMs are complex whose response surfaces always display strong nonlinearity and

603   discontinuity, casting a challenge to surrogate modeling. In this section, we consider the

604   strategies of physics-informed learning and increase of training data to improve the surrogate

605   accuracy. We conduct two corresponding experiments to investigate our method's performance

606   in application of these two strategies. In experiment I, we divide the parameter space into two

607   parts producing zero GPPs and nonzero GPPs, and we use 20 training data to build surrogates of

608   the 42660 GPPs in the regime generating nonzero GPP samples. In experiment II, we build the

609   surrogates of the 42660 GPPs in the original parameter domain (Figure 3), but with increasing

610   training data of 200 and 1000.

611   We use the results of Case I as a baseline to investigate our method's performance in the

612   two experiments. Figure 12 shows averaged R^2 scores over 30 years at the 1422 locations in

613   experiment I. The figure indicates that without zero GPPs our method can produce a very

614   accurate surrogate at all locations with a uniformly high R^2 score of 0.98. Building the surrogates

615   in the subdomain without zero GPPs not only significantly improves the prediction accuracy in

616   locations originally having poor fit in Case I, but also further improves the prediction accuracy in

617   locations which already have a good fit in Case I. For example, the R^2 score is dramatically

618   improved from 0.79 to 0.97 at location 1345, from 0.96 to 0.99 at location 1046, and from 0.91

619   to 0.98 at location 428. As shown in Figure 13, the NN almost perfectly reproduces sELM

620   simulations at these 3 locations. Experiment I indicates that physics-informed domain

621   decomposition can be a good strategy to improve surrogate accuracy. For smooth problems (e.g.,

622   no sharp jumps from non-zeros to zeros in response surfaces), our method can build a very

623   accurate surrogate model based on a few training data.

624   Figure 14 shows averaged R^2 scores over 30 years at 1422 locations based on 200 and

625   1000 training data in experiment II. The figure indicates that an increase of training data greatly

626   enhances NN prediction accuracy. Adding 10 folds additional data from Ntrain=20 to

627   Ntrain=200, the overall R^2 score improves from 0.93 to 0.98; further increasing Ntrain to 1000,

628   the averaged R^2 score is up to 0.993 with the worst value of 0.96. Although we observe similar

629   nonuniform performance among locations in Figure 14 as in Figure 9, where the locations with

630   zero GPPs have smaller R^2 scores than others, increasing Ntrain significantly improves the

631   accuracy at all locations, especially those originally having poor fits in Case I. For example,

632 when Ntrain=200, most blue-circled locations have R^2 scores above 0.95 and for Ntrain=1000,

633 the R^2 scores at these blue-circled locations are above 0.985 in comparison to the values below

634 0.9 when Ntrain=20. In the examination of the 3 individual locations by comparing Figure 10

635 and Figure 15, we see that at the location of 1046, an increase of Ntrain enables the NN to

636 perfectly predict sELM simulations with negligible MSEs. Even for the location 428 with zero

637 GPPs, more training data can capture the discontinuous behavior better with R^2 score of 0.99 and

638 MSE of 0.003 when Ntrain=1000. The worst location happens at 1345 for all cases due to its

639 highly changed atmospheric drivers. Even so, the increase of Ntrain can still dramatically

640 enhance the NN's capability in simulating the difficult response surface. Experiment II indicates

641 that increasing training data is able to significantly improve the surrogate accuracy. Our method

642 scales well with the increase of training data and greatly improves prediction accuracy as Ntrain

643 increases.

644 The analysis of the two experiments suggests that our method is data-efficient for

645 continuous problems. To improve the surrogate accuracy in discontinuous and highly nonlinear

646 problems, we can use the physical-informed domain decomposition to focus on the continuous

647 and smooth regions of the response surface. If the discontinuity is the inherent feature of the

648 underlying function that we need to surrogate, an increase of training data would be a good

649 solution for surrogate accuracy improvement.

650 Having built a surrogate system of many GPP variables over large spatial and temporal

651 domains provides great flexibility and possibility for subsequent predictive analytics tasks. For

652 example, the surrogate model can be used for analyzing sensitivities of model parameters to any

653 set of spatial and temporal GPP variables, and for parameter optimization and uncertainty

654 quantification based on a single-site or multiple-site, a single-year or multiple-year GPP

655   observations using any defined objective functions. In addition, with the newly collected

656   observations from additional sites or further time periods, we can use the same surrogate system

657   for analysis as long as the QoIs are within the surrogate simulation ranges. In the future study,

658   we will pursue the data-model integration using the constructed surrogate system.

659   **5   Conclusions**

660   In this work, we develop an SVD-enhanced, Bayesian-optimized, and NN-based surrogate

661   method to improve the computational efficiency of large-scale surrogate modeling, so as to

662   advance model-data integration studies in Earth system model simulations. Our method is data

663   efficient in the fact that only 20 model simulations are needed to build an accurate surrogate

664   system. This is a promising result because large Earth system model ensembles are always

665   computationally infeasible, and 20 is a reasonable and affordable number of simulations to

666   consider. In addition, our method is general purpose and can be efficiently applied to a wide

667   range of Earth system problems with different spatial scales (local, regional, or global) at

668   different simulation periods. It is super effective for smooth problems and scaled well for highly

669   nonlinear and discontinuous problems.

670   We apply our surrogate method to a regional ecosystem model. The results indicate that

671   using only 20 model runs, we can build an accurate surrogate system of 42660 spatially- and

672   temporally-varied GPPs with the R^2 score of 0.93 and MSE of 0.02. For locations with robust

673   vegetation growth across the ensemble, our method can almost perfectly predict the model

674   simulations with the R^2 score of 0.96. For locations with low vegetation growth for some

675   parameter samples and large variation in atmospheric drivers that cause discontinuous response

676   surfaces, using physics-informed domain decomposition or the increase of training samples, our

677   method can produce accurate predictions with the R^2 score of 0.97 and 0.96, respectively. This

678 application demonstrates our method's capability in accurately reproducing expensive model

679 simulations based on a few parallel model runs.

680 **Data availability**

681 All the data used in this study are model simulation data, which can be generated by running

682 the sELM.

683 **Code availability**

684 sELM is presented in its 1.0 version, which is realized in the Python language. It is an open-

685 source   computer   code   which   can   be   accessed   freely   from

686 https://github.com/dmricciuto/OSCM_SciDAC/tree/master/models/simple_ELM.   The   source

687 code of surrogate modeling using machine learning techniques can be provided upon request via

688 lud1@ornl.gov.

689 **Author contribution**

690 Dan Lu developed the methods and carried them out. Daniel Ricciuto developed the model

691 code and performed the model simulations. Dan Lu prepared the manuscript with contributions

692 from the coauthor.

693 **Acknowledgments**

694 Primary support for this work was provided by the Scientific Discovery through Advanced

695 Computing (SciDAC) program, funded by the U.S. Department of Energy (DOE), Office of

696 Advanced Scientific Computing Research (ASCR) and Office of Biological and Environmental

697 Research (BER). Additional support was provided by BER's Terrestrial Ecosystem Science

698 Scientific Focus Area (TES-SFA) project. The authors are supported by Oak Ridge National

699 Laboratory, which is supported by the DOE under Contract DE-AC05-00OR22725.

700 **References**

701 Agarap, A. F. M.: Deep learning using Rectified Linear Units (ReLU),

702   https://arxiv.org/pdf/1803.08375, 2018.

703 Bardenet, R. and Kegl, B.: Surrogating the surrogate: accelerating Gaussian Process optimization

704   with mixtures, In ICML, 2010.

705 Basu A., De, S., Mukherjee, A., and Ullah, E.: Convergence guarantees for rmsprop and adam in

706   nonconvex optimization and their comparison to nesterov acceleration on autoencoders,

707   arXiv preprint arXiv:1807.06766, 2018.

708 Bergstra J. S., Bardenet, R., Bengio, Y., and Kegl, B.: Algorithms for hyperparameter

709   optimization, NIPS 24, 2546-2554, 2011.

710 Bergstra J., and Bengio, Y.: Random search for hyper-parameter optimization, Journal of

711   Machine Learning Research, 13(1): 281-305, 2012.

712 Bergstra, J., Yamins, D., and Cox, D. D.: Hyperopt: A Python library for optimizing the

713   hyperparameters of machine learning algorithms, In Proceedings of the 12th Python in

714   Science Conference, 13-20, 2013.

715 Bottou, L.: Stochastic gradient descent tricks, Neural networks: tricks of the trade: 2nd edition,

716   Springer Berlin Heidelberg, 2012.

717 Bilionis, I., Drewniak, B. A., and Constantinescu, E. M.: Crop physiology calibration in the

718   CLM, Geosci. Model Dev., 8, 1071-1083, 2015.

719 Fox, A., Williams, M., Richardson, A. D., Cameron, D., Gove, J. H., Quaife, T., Ricciuto, D.,

720   Reichstein, M., Tomelleri, E., Trudinger, C. M., and Van Wijk, M. T.: The REFLEX

721   project: Comparing different algorithms and implementations for the inversion of a

722   terrestrial ecosystem model against eddy covariance data, Agric. For. Meteorol., 149,

723   1597-1615, 2009.

724 Gong, W., Duan, Q., Li, J., Wang, C., Di, Z., Dai, Y., Ye, A., and Miao, C.: Multiobjective

725   parameter optimization of community land model using adaptive surrogate modeling,

726   Hydrol. Earth Syst. Sci., 19, 2409-2425, 2015.

727 Huang, M., Ray, J., Hou, Z., Ren, H., Liu, Y., and Swiler, L.: On the applicability of surrogate-

728   based Markov chain Monte Carlo-Bayesian inversion to the Community Land Model:

729   Case studies at flux tower sites, J. Geophys. Res. Atmos., 121, 7548-7563,

730   doi:10.1002/2015JD024339, 2016.

731 Kim, H.: Global Soil Wetness Project Phase 3 Atmospheric Boundary Conditions (Experiment

732   1). Data Integration and Analysis System (DIAS), https://doi.org/10.20783/DIAS.501,

733   2017.

734 Kingma, D. P., and Ba, J.: Adam: a Method for Stochastic Optimization, International

735   Conference on Learning Representations, 1-13, 2015.

736 Lu, D., Ricciuto, D., Walker, A., Safta, C., and Munger W.: Bayesian calibration of terrestrial

737   ecosystem models: a study of advanced Markov chain Monte Carlo methods,

738   Biogeosciences, 14, 4295-4314, 2017.

739 Lu, D., Ricciuto, D., Stoyanov, M., and Gu, L.: Calibration of the E3SM land model using

740   surrogate-based global optimization. Journal of Advances in Modeling Earth Systems,

741   10. https://doi.org/10.1002/2017MS001134, 2018.

742 Luo, J. and Lu W.: Comparison of surrogate models with different methods in groundwater

743   remediation process, Journal of Earth System Science, 123(7), 1579-1589, 2014.

744 Müller, J., Paudel, R., Shoemaker, C. A., Woodbury, J., Wang, Y., and Mahowald, N.: CH4

745   parameter estimation in CLM4.5bgc using surrogate global optimization, Geosci. Model

746   Dev., 8, 3285-3310, 2015.

747 Niranjan, S., Krause, A., Kakade, A., and Seeger, M.: Gaussian process optimization in the

748   bandit setting: No regret and experimental design. In Proceedings of the 27th

749   International Conference on Machine Learning, 2010.

750 Oleson, K. W., et al.: Technical description of version 4.5 of the Community Land Model

751   (CLM). (NCAR Tech. Note NCAR/TN-5031STR, 420 pp. Boulder, CA: National

752   Center for Atmospheric Research, https://doi.org/10.5065/D6RR1W7M, 2013.

753 Ray, J., Hou, Z., Huang, M., Sargsyan, K., and Swiler, L.: Bayesian calibration of the

754   Community Land Model using surrogates, SIAM/ASA J. Uncertain. Quantif., 199-233,

755   doi:10.1137/140957998, 2015.

756 Razavi, S., Tolson, B. A., and Burn, D. H.: Review of surrogate modeling in water resources,

757   Water Resour. Res., 48, W07401, doi:10.1029/2011WR011527, 2012.

758 Ricciuto, D., Sargsyan, K., and Thornton, P.: The impact of parametric uncertainties on

759   biogeochemistry in the E3SM land model. Journal of Advances in Modeling Earth

760   Systems, 10, 297-319, 2018.

761 Sargsyan, K., Safta, C., Najm, H. N., Debusschere, B., Ricciuto, D. M., and Thornton, P.E.:

762   Dimensionality reduction for complex models via Bayesian compressive sensing, Int. J.

763   Uncert. Quant., 4, 63-93, 2014.

764 Shahriari, B., Swersky, K., Wang, Z., Adams, R. P., and de Freitas, N.: Taking the Human Out of

765   the Loop: A Review of Bayesian Optimization, Proc. IEEE 104 (1): 148-175,

766   doi:10.1109/jproc.2015.2494218, 2016.

767 Snoek, J., Larochelle, H., and Adams, R. P.: Practical Bayesian optimization of machine learning

768   algorithms, in 26th Annual Conference on Neural Information Processing Systems,

769   2960-2968, 2012.

770   Williams, M., Schwarz, P. A., Law, B. E., Irvine, J., and Kurpius, M.: An improved analysis of

771   forest carbon dynamics using data assimilation, Global Change Biol., 11, 89-105, 2005.

772   Viana, F. A., Simpson, T.W., Balabanov, V., and Toropov, V.: Metamodeling in

773   multidisciplinary design optimization: How far have we really come?, AIAA J., 52(4),

774   670-690, 2014.

775   Yegnanarayana B.: Artificial neural networks, PHI Learning Pvt. Ltd, 2009.
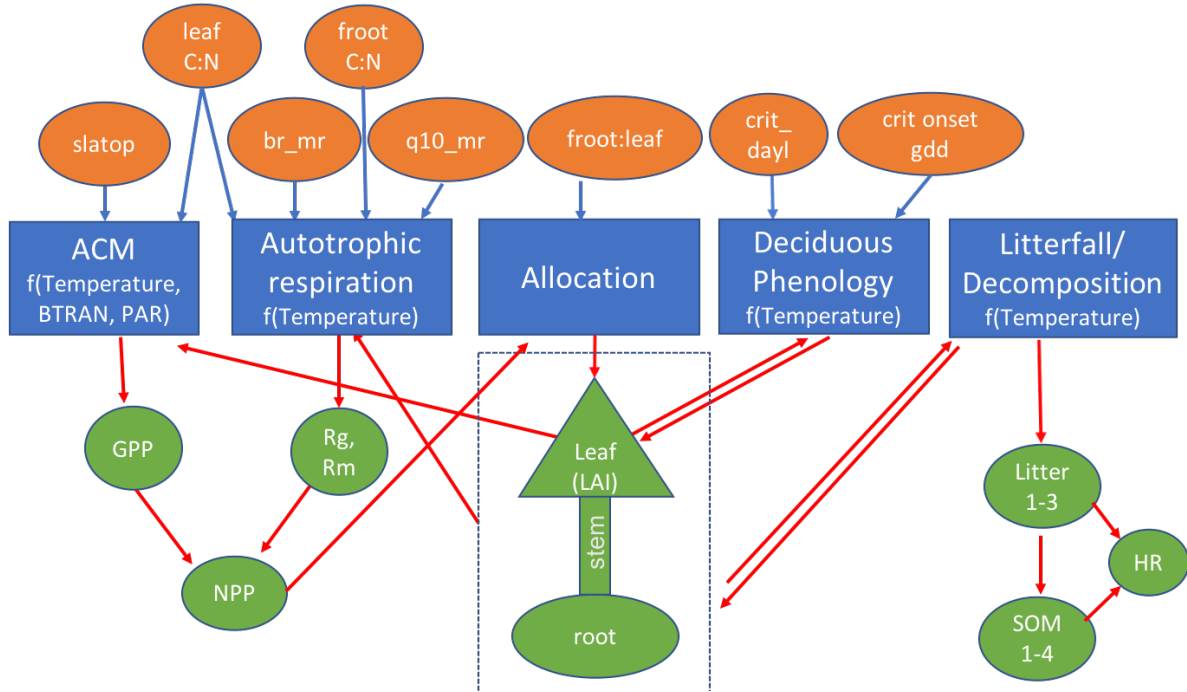
777

778 Figure 1. Schematic of sELM, where processes are shown using blue boxes with dependencies
779 on environmental data, 8 uncertain parameter inputs are listed in orange ovals, and model state
780 variables are indicated by green shapes. Parameters are input to one or more processes as
781 indicated by blue arrows. Model state variables may be outputs for some processes and input for
782 other processes as indicated by red arrows.

783

784
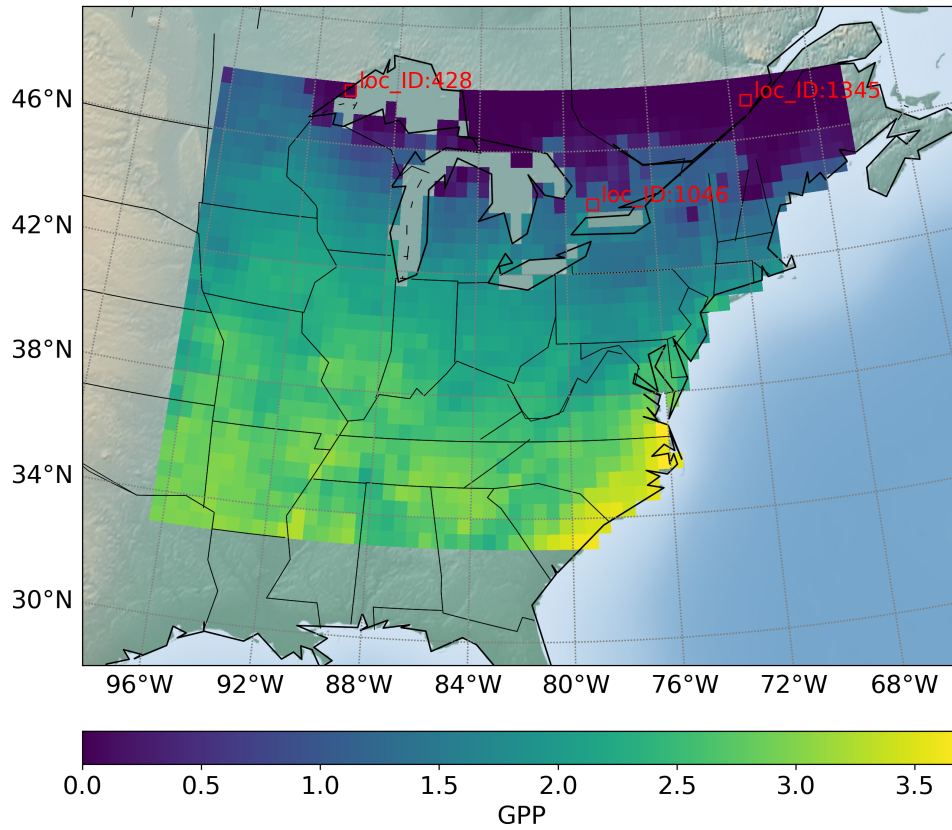
Figure 2. Locations of interest for which we build surrogates of GPP (gC/m^2/day) variables; total 1422 locations are considered. The figure shows the sELM simulated annual GPP based on one parameter sample.
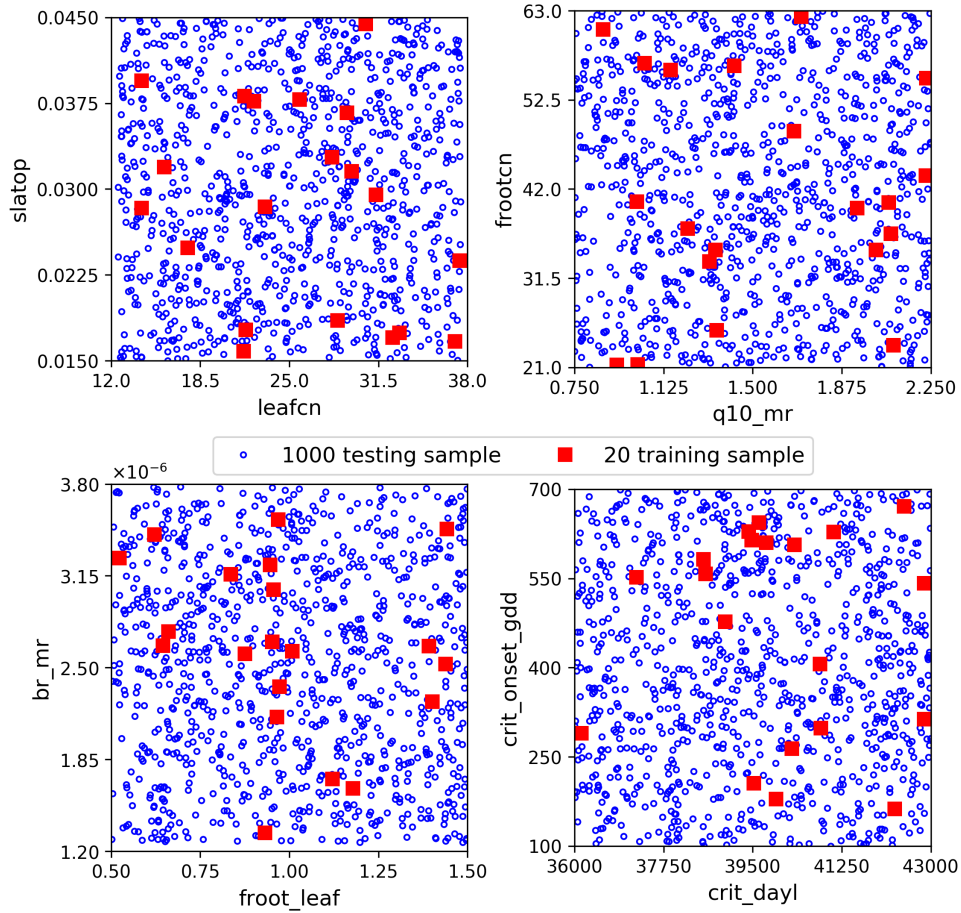
790

791   Figure 3. We consider 8 uncertain parameter inputs whose ranges are shown as axis limits. The
792   20 training and 1000 testing data are randomly drawn from the parameter space.

793

794
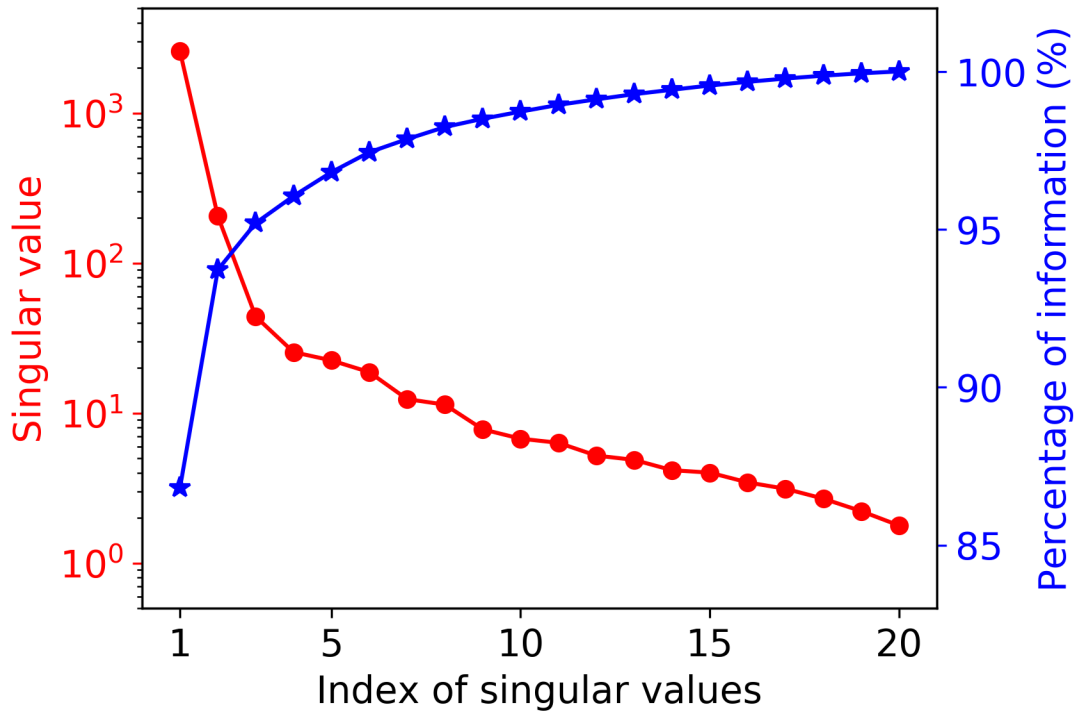
Figure 4. Singular value decay and the information contained in the first largest singular values. The top 5 singular values contain 97% information of training data matrix with 42660 GPP variables and 20 samples.

798
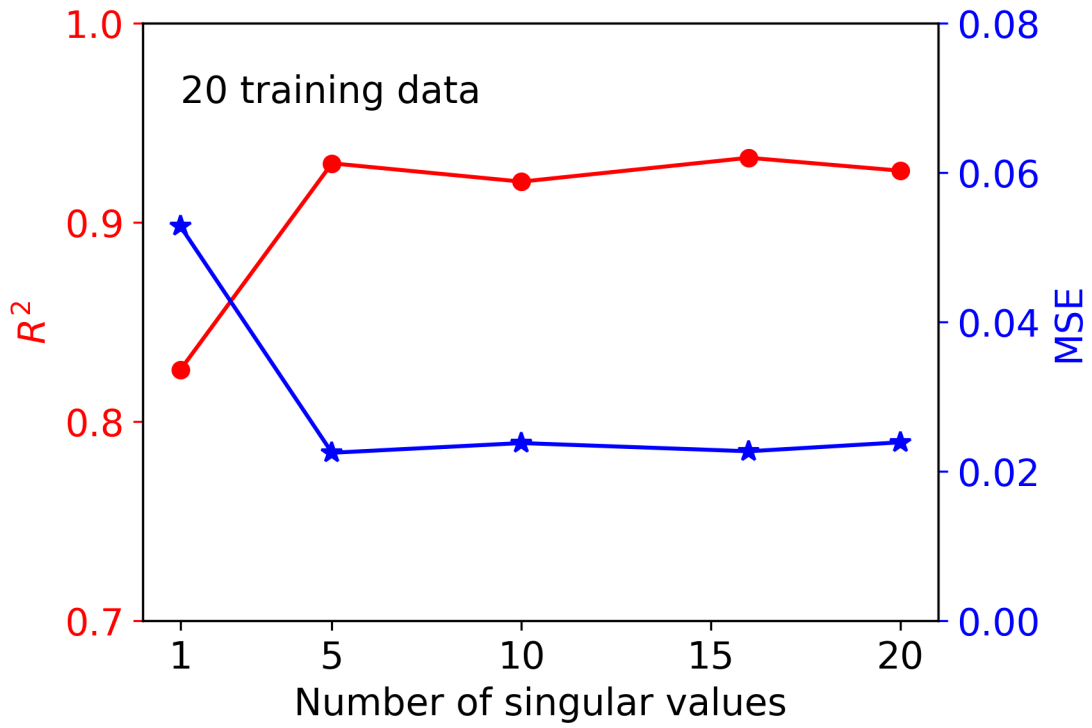
Figure 5. Performance of the NNs trained by 20 data with considering the different number of singular value coefficients after SVD.
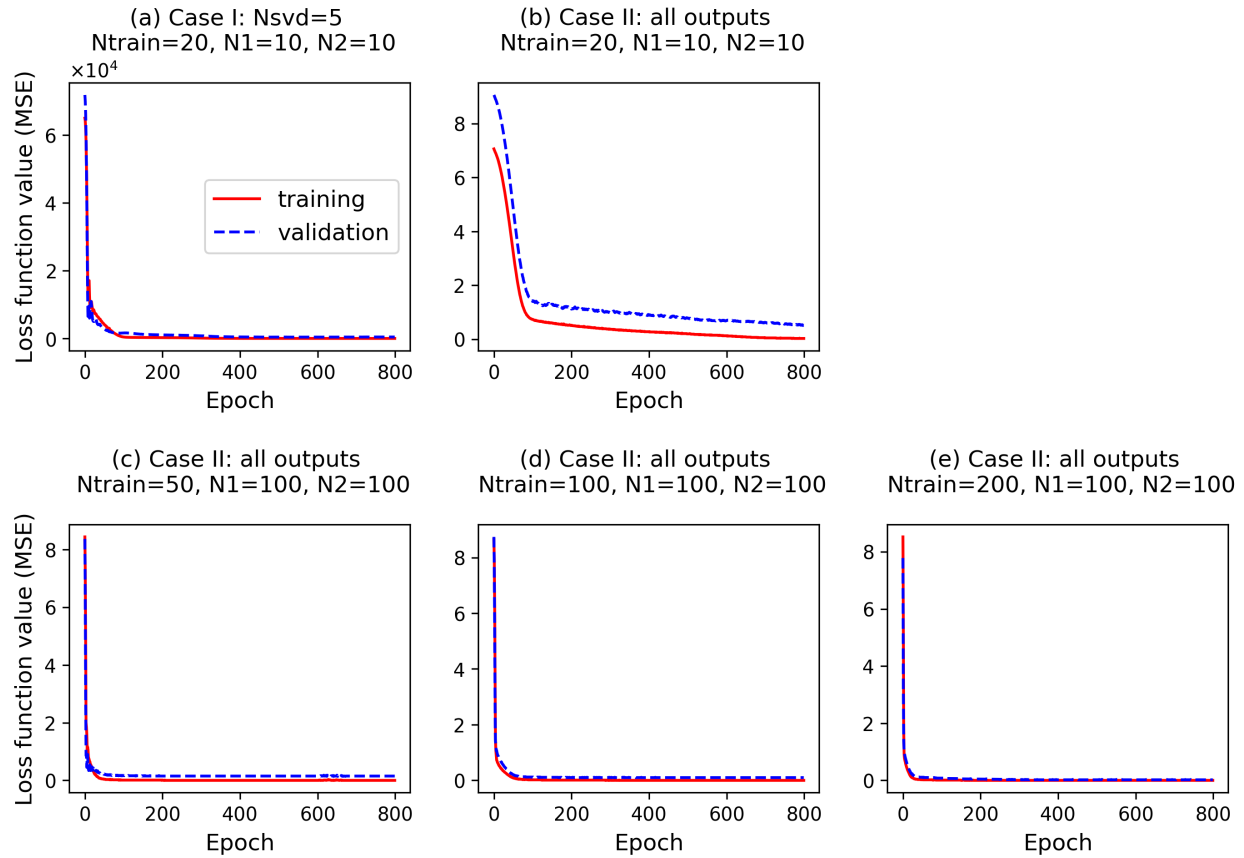
803

804 Figure 6. Changes of loss function values along epochs for training and validation data (a) in
805 Case I which builds surrogates of the 5 singular value coefficients with a simple NN (two hidden
806 layers and each layer has 10 nodes, N1=N2=10) based on 20 training data (Ntrain=20), and (b-e)
807 in Case II which builds surrogates of all outputs with different NN architectures and different
808 training data size.

809

810
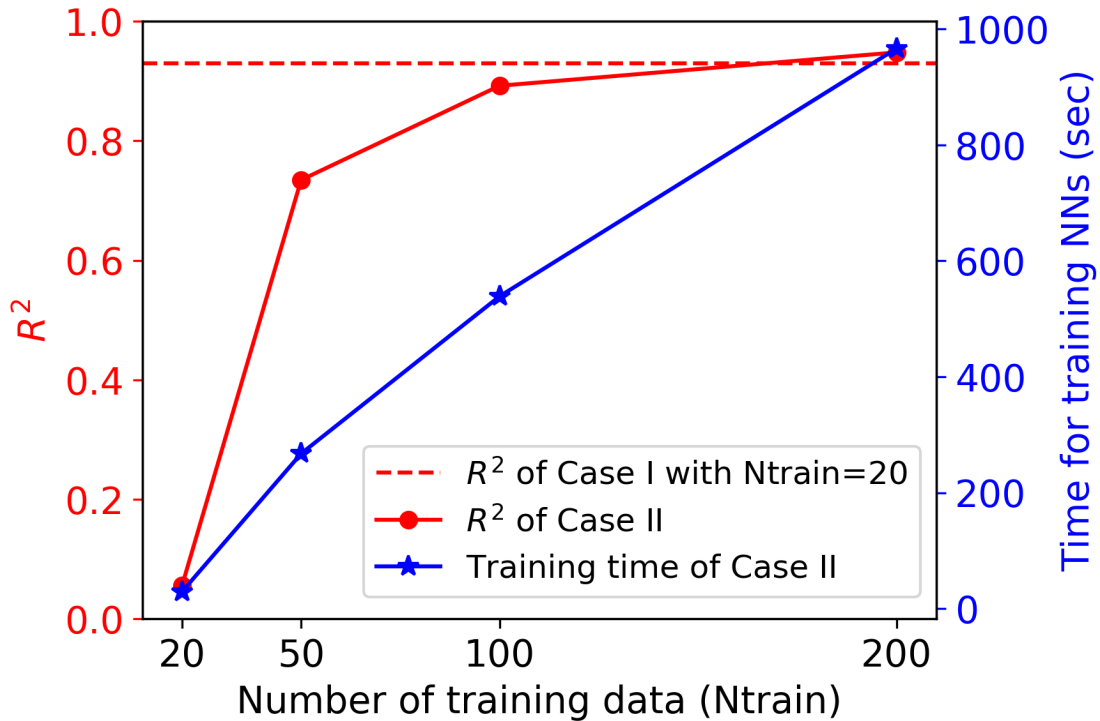
Figure 7. Comparison of NN performance between Case I: building surrogates of 5 singular value coefficients (Nsvd=5) after SVD based on 20 training data (red dashed line) and Case II: building surrogates for all outputs directly with different numbers of training data (red solid line). Each training data represents one sELM simulation. The right y-axis shows the time in training the NN in Case II. The time for training the NN in Case I is 4 seconds.

816
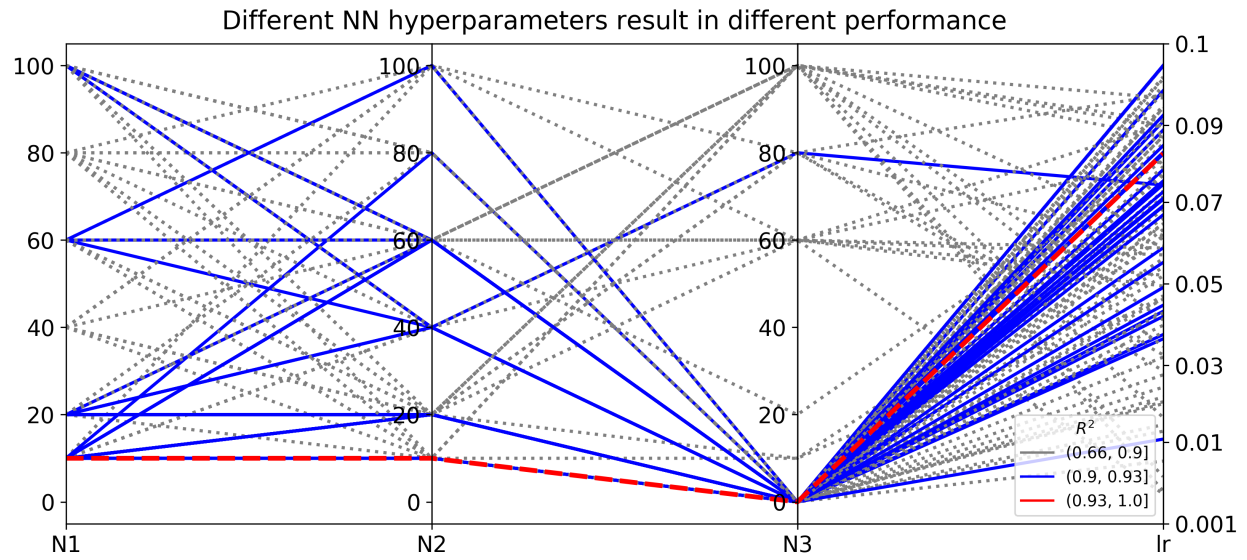
817

818 Figure 8. Different sets of NN hyperparameters result in different R^2 score in evaluating the 1000
819 test data. Nl is the number of nodes in hidden layer l, where l=1, 2, and 3. lr is the learning rate
820 of Adam algorithm for NN weights optimization.

821
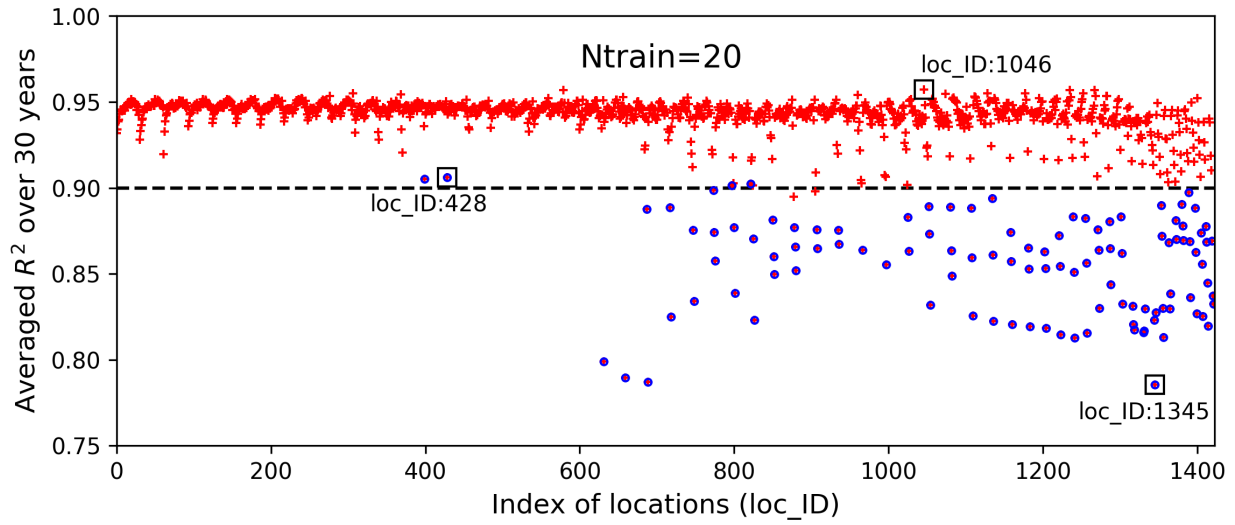
822

823 Figure 9. Averaged R^2 scores over 30 years at 1422 locations in evaluating the 1000 test data
824 based on 20 training samples, where the blue circles identify the locations having zero GPP
825 simulations.

826
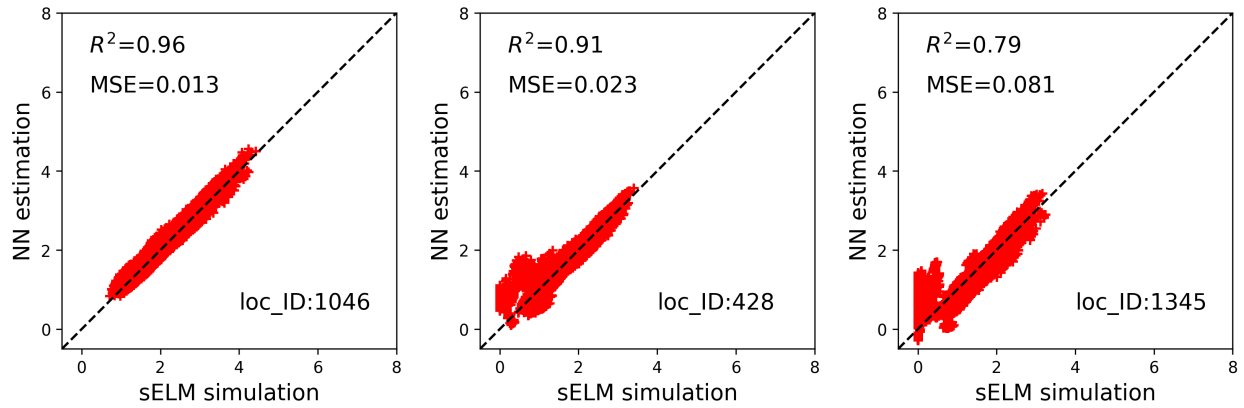
Figure 10. Simulations of annual GPPs (gC/m^2/day) from sELM and NN-based surrogate
model in evaluating 1000 test data for 30 years at 3 locations, where the NN is trained by 20 data
using our method.
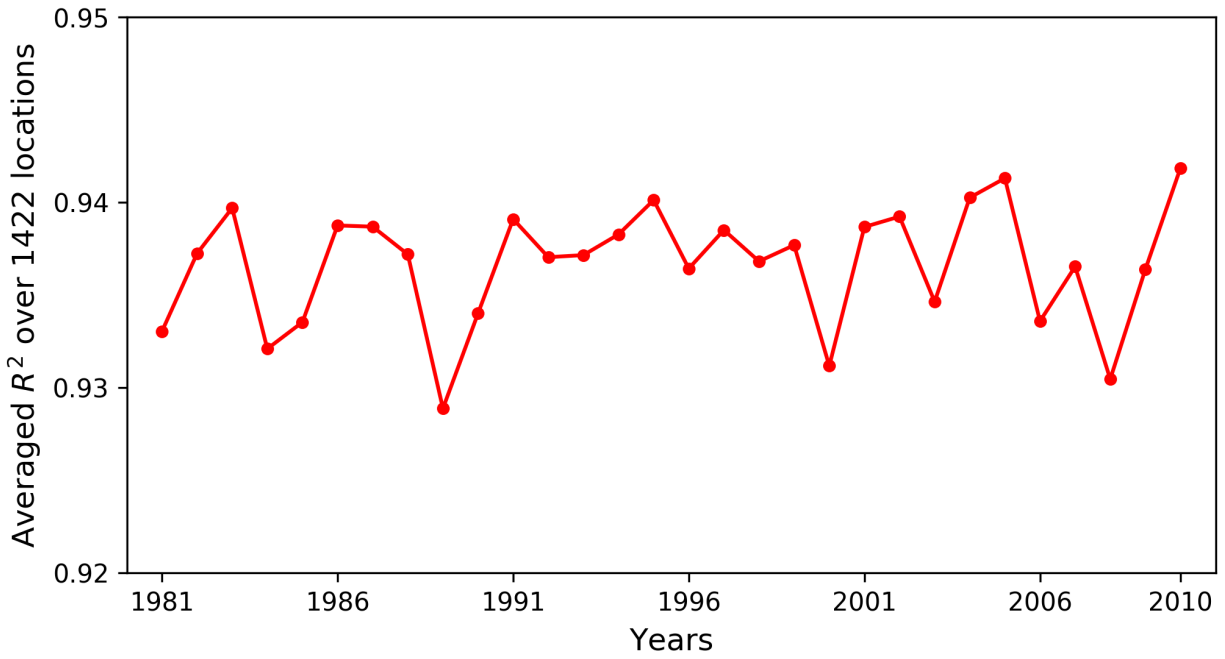
832

833   Figure 11. Averaged R^2 scores over 1422 locations at 30 years in evaluating the 1000 test data.

834
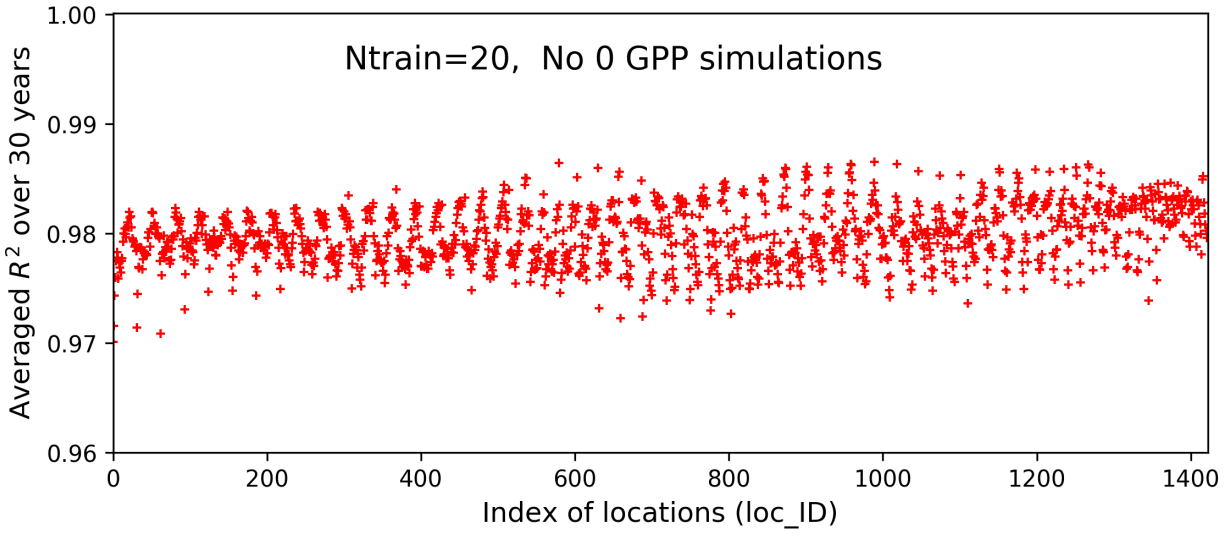
835

836   Figure 12. Averaged R^2 scores over 30 years at 1422 locations in evaluating the 1000 test data
837   based on 20 training data in experiment I where the samples are generated in a subdomain of the
838   parameter space without zero GPP simulations. The averaged R^2 score is 0.98.

839
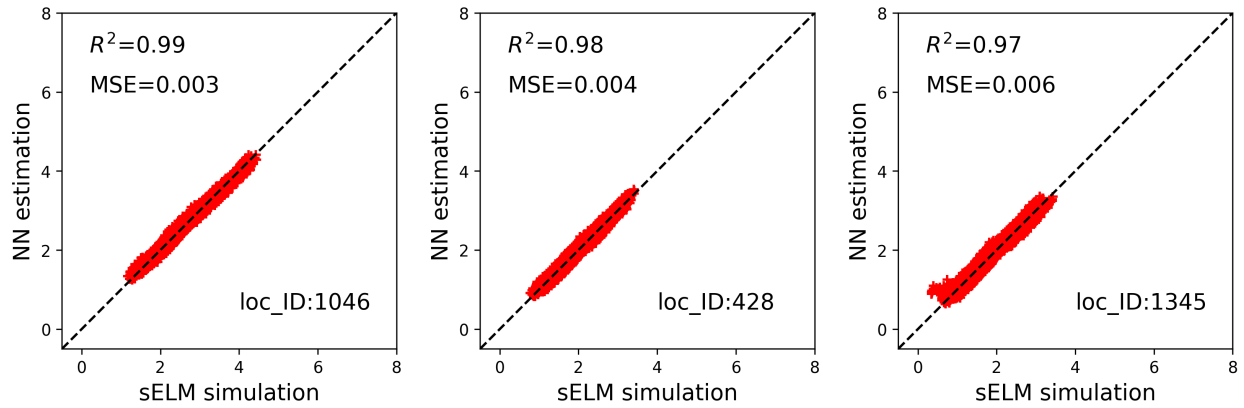
840

841 Figure 13. Simulations of annual GPPs (gC/m^2/day) from sELM and NN-based surrogate
842 model in evaluating 1000 test data for 30 years at 3 locations in experiment I where the samples
843 are generated in a subdomain of the parameter space without zero GPP simulations.

844

845

846
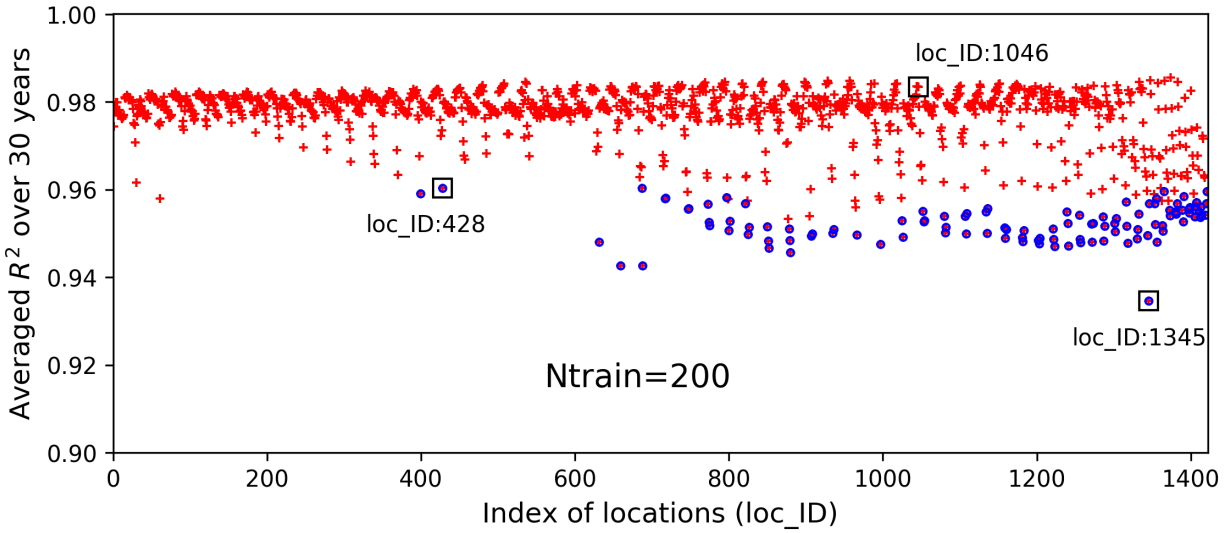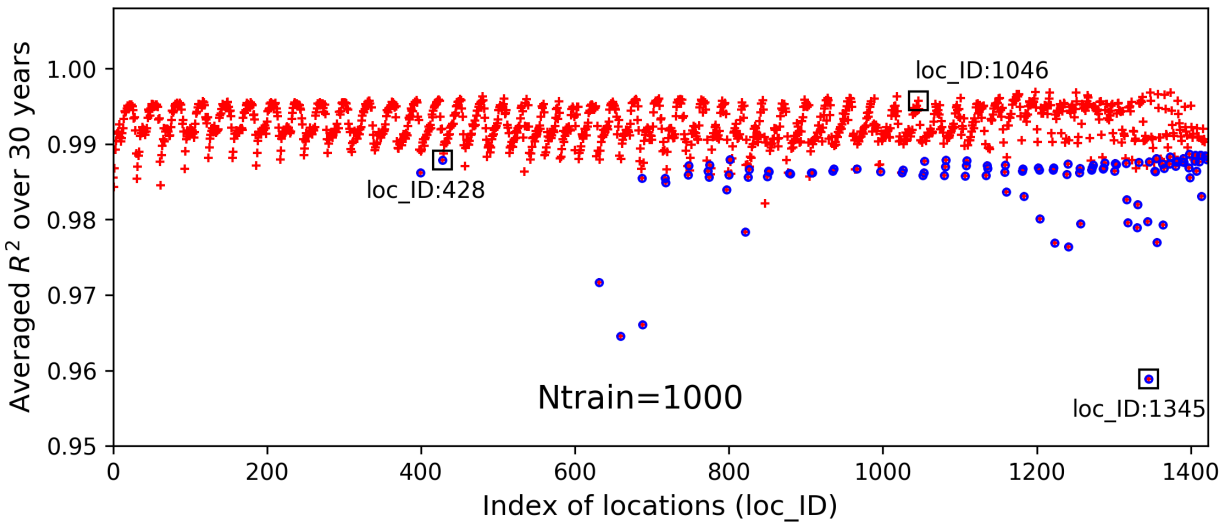
Figure 14. Averaged R^2 scores over 30 years at 1422 locations in evaluating the 1000 test data based on 200 and 1000 training samples, where the blue circles identify the locations having zero GPP simulations.

847
848
849

850
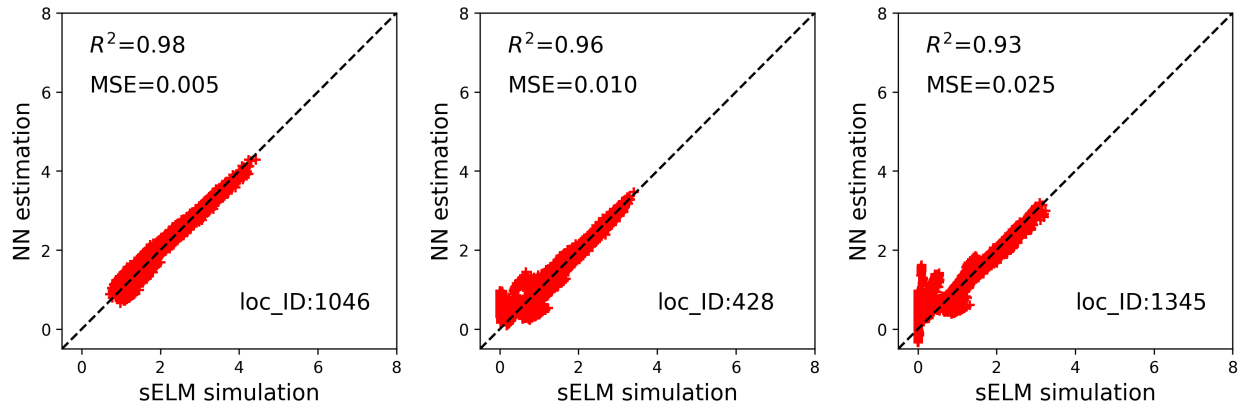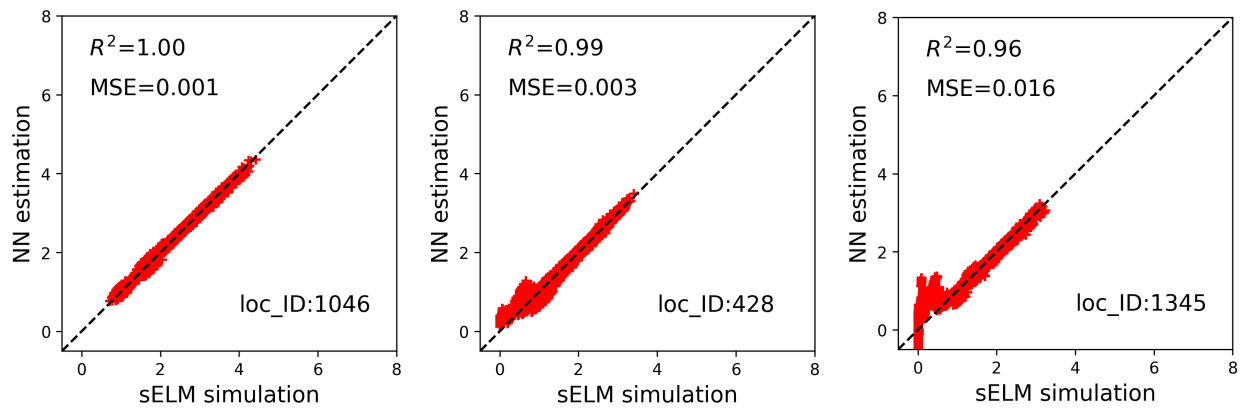
Figure 15. Simulations of annual GPPs (gC/m^2/day) from sELM and NN-baed surrogate model in evaluating 1000 test data for 30 years at 3 locations, where the NN is trained by 200 and 1000 data.